ELSEVIER

Biophysical Chemistry 69 (1997) 125–135

Biophysical Chemistry

Analysis of differential scanning calorimetry data for proteins Criteria of validity of one-step mechanism of irreversible protein denaturation

Boris I. Kurganov [a,*], Arkady E. Lyubarev [a], Jose M. Sanchez-Ruiz [b], Valery L. Shnyrov [c]

[a] *A.N. Bakh Institute of Biochemistry, Russian Academy of Sciences, Leninsky pr. 33, Moscow 117071, Russian Federation*
[b] *Departamento de Química-Física, Facultad de Ciencias e Instituto de Biotecnología, Universidad de Granada, E-18071 Granada, Spain*
[c] *Departamento de Bioquímica y Biología Molecular, Universidad de Salamanca, Avenida del Campo Charro, s / n, 37007 Salamanca, Spain*

Received 27 January 1997; revised 23 May 1997; accepted 27 May 1997

Abstract

We consider in this work the analysis of the excess heat capacity C_p^{ex} versus temperature profiles in terms of a model of thermal protein denaturation involving one irreversible step. It is shown that the dependences of ln C_p^{ex} on $1/T$ (T is the absolute temperature) obtained at various temperature scanning rates have the same form. Several new methods for estimation of parameters of the Arrhenius equation are explored. These new methods are based on the fitting of theoretical equations to the experimental heat capacity data, as well as on the analysis of the dependence $d(\ln C_p^{ex})/d(1/T)$ on $1/T$. We have applied the proposed methods to calorimetric data corresponding to the irreversible thermal denaturation of *Torpedo californica* acetylcholinesterase, cellulase from *Streptomyces halstedii* JM8, and lentil lectin. Criteria of validity for the one-step irreversible denaturation model are discussed. © 1997 Elsevier Science B.V.

Keywords: Protein denaturation; Differential scanning calorimetry; Acetylcholinesterase; Cellulase; Lentil lectin

1. Introduction

Differential scanning calorimetry (DSC) is a powerful technique to characterize the energetics and mechanisms of temperature-induced conformational changes of biological macromolecules [1–12]. In cases of reversible denaturation, the equilibrium thermodynamics analysis of the DSC thermograms allows us to check the two-state character of the process and, in the case of non-two-state denaturation, to determine the number and to develop a thermodynamic characterization of the significantly populated intermediate states. This latter situation is more likely to occur with complex, multidomain proteins and some studies suggest that information on the domain–domain interactions may be obtained from DSC data [13,14]. However, the thermal denaturation of many proteins is irreversible due to the occurrence of 'side' process such as aggregation, autolysis, chemical alterations of amino acid residues, etc. [15]. In most cases, analysis of DSC data for

* Corresponding author. Fax: +7-095-954-2732; e-mail: inbio@glas.apc.org

protein irreversible denaturation must be carried out on the basis of specific kinetic models, which would lead to the kinetic parameters of the denaturation process and their temperature-dependence.

The goal of the present paper is to explore some new approaches to the analysis of DSC data for protein irreversible denaturation, paying special attention to the criteria for the validity of the one-step, irreversible denaturation mechanism. Analysis of experimental data corresponding to the irreversible denaturation of *Torpedo californica* acetylcholinesterase, lentil lectin, and cellulase from *Streptomyces halstedii* JM8 will be used for illustration of applicability of the new approaches.

2. Model

The simplest model of irreversible denaturation of a protein is a monomolecular transformation of a native protein (N) to the irreversibly denatured state (D) according to a first-order rate constant, k:

$$N \xrightarrow{k} D \tag{1}$$

The analysis of DSC profiles in terms of this model was first discussed by Freire et al. [10], Sanchez-Ruiz [11,12], and Sanchez-Ruiz et al. [16] and, subsequently, the model has been used for the quantitative description of thermal denaturation of a number of proteins [16–21]. This 'two-state irreversible model' has been shown to be a limiting case of more realistic Lumry and Eyring model in which the reversible unfolding of the protein is followed by a kinetically-controlled alteration of an unfolded or partially unfolded state to yield an irreversible denatured state that is unable to fold back to the native structure [11].

The rate constant k is assumed to follow the Arrhenius law:

$$k = A\exp(-E_a/RT) = \exp\{(E_a/R)(1/T^* - 1/T)\} \tag{2}$$

where A is the pre-exponential multiplier, E_a is the experimental energy of activation, T is the absolute temperature, T^* is the temperature at which $k = 1$ min^{-1}. It should be noted that $1/T^*$ is the ratio $(\ln A)/(E_a/R)$. Note also that, given the comparatively narrow temperature range of the DSC transitions, a description of k in terms of transition state theory would be phenomenologically equivalent to the Arrhenius equation used here. In fact, activation enthalpies and entropies may be easily calculated from the values of A and E_a by using well-known equations.

The rate equation for this model is:

$$d[N]/dt = -k[N] \tag{3}$$

If temperature is a variable parameter and the rate of the variation of temperature is constant ($dT/dt \equiv v$, t is time), Eq. (3) acquires the following form:

$$d[N]/dT = -(1/v)k[N] \tag{4}$$

Integration of this equation gives the expression for the relative amount of the N state, γ_N, as a function of temperature ($\gamma_N \equiv [N]/[N]_0$, where $[N]_0$ is the concentration of the N state at the initial temperature of the scanning experiment, T_0):

$$\gamma_N = \exp\left\{-\frac{1}{v}\int_{T_0}^{T}\exp\left[\frac{E_a}{R}\left(\frac{1}{T^*}-\frac{1}{T}\right)\right]dT\right\} \tag{5}$$

If the native state (N) is taken as a reference state, the excess of enthalpy $\langle \Delta H \rangle$ and excess heat capacity C_p^{ex} are given by:

$$\langle \Delta H \rangle = (1 - \gamma_N)\Delta H \tag{6}$$

(ΔH is the enthalpy difference between the denatured and native states),

$$C_p^{ex} = \frac{\partial(\langle \Delta H \rangle)}{\partial T} = \frac{1}{v}\Delta H \exp\left\{\frac{E_a}{R}\left(\frac{1}{T^*}-\frac{1}{T}\right)\right\} \times \exp\left\{-\frac{1}{v}\int_{T_0}^{T}\exp\left[\frac{E_a}{R}\left(\frac{1}{T^*}-\frac{1}{T}\right)\right]dT\right\} \tag{7}$$

where ΔH is the denaturation enthalpy (the enthalpy of the denatured state taking the native state as reference). It must be noted that Eq. (7) assumes that ΔH is constant within the narrow temperature range of the DSC transition; as a result, Eq. (7) is intended to describe the excess heat capacity profiles obtained by using the so-called chemical baseline as reference level (for details on baseline corrections, see Ref. [12]).

The total heat absorbed (calculated by integration of the C_p^{ex} versus temperature profile) is equal to the denaturation enthalpy change ΔH. In the following, we shall designate the ΔH value as Q_t and the

$\langle \Delta H \rangle$ value as Q. In this case, Eq. (7) may be transformed as follows:

$$C_p^{ex} = (1/v)(Q_t - Q) \times \exp\{(E_a/R)(1/T^* - 1/T)\} \quad (8)$$

The plot of C_p^{ex} versus T is an asymmetric curve passing through a maximum with temperature (see, for example, [10–12,16] and Section 5 of the present paper).

Five methods of E_a estimation were proposed by Sanchez-Ruiz et al. These methods have been widely employed and are described in detail in several places [11,12,16,21].

One of the methods is based on the construction of the linear dependence $\ln [vC_p^{ex}/(Q_t - Q)]$ versus $1/T$ according to

$$\ln\left[vC_p^{ex}/(Q_t - Q)\right] = \ln A - (E_a/R)(1/T) \quad (9)$$

3. New graphical anamorphoses

Fig. 1A shows the theoretical dependences of C_p^{ex} on temperature calculated by us for the one-step irreversible denaturation mechanism (1) by Eq. (7) at selected values of ΔH, E_a, and T^*. These dependences are presented in coordinates $\{\ln C_p^{ex};\ 1/T\}$. At sufficiently high values of $1/T$, the slope of the curves approaches $-(E_a/R)$. Of special interest is that the $\ln C_p^{ex}$ versus $1/T$ curves obtained at various values of the scanning rate v have the same form. This may be proved by the following way. If one brings together the maximum points of the dependences of $\ln C_p^{ex}$ on $1/T$, these dependences fit into the common curve. This result suggests that the identity of the shape of $\ln C_p^{ex}$ versus $1/T$ curves obtained at various values of the scanning rate may be used as a criterion of validity of the mechanism of protein denaturation involving one irreversible step.

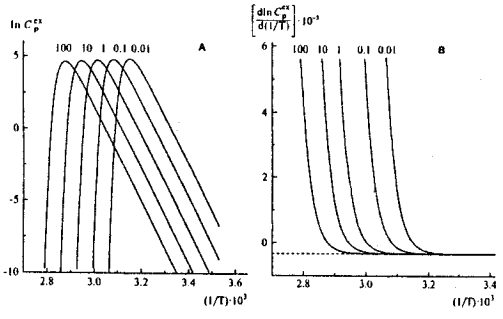

Fig. 1. The theoretical dependences of $\ln C_p^{ex}$ on the reciprocal value of absolute temperature (A) and the dependences of $d(\ln C_p^{ex})/d(1/T)$ on $1/T$ (B) for the one-step irreversible denaturation mechanism (Eq. (1)) calculated from Eq. (7) at $\Delta H = 1000$ kJ/mol, $E_a = 274$ kJ/mol, $T^* = 335.6$ K, and the various values of the temperature scanning rate v in K/min (number near the curves).

The modern methods of registration of DSC curves provide a sufficiently large number of points on the C_p^{ex} versus temperature profiles. This circumstance allows such dependences to be presented in a differential form. In particular, the dependences of $d(\ln C_p^{ex})/d(1/T)$ on $1/T$ can be constructed. The theoretical dependences of $d(\ln C_p^{ex})/d(1/T)$ on $1/T$ for the model under discussion have the following form:

$$d(\ln C_p^{ex})/d(1/T) = (1/v)T^2 \times \exp\{(E_a/R)(1/T^* - 1/T)\} - E_a/R \quad (10)$$

Fig. 1B shows the theoretical dependences of $d(\ln C_p^{ex})/d(1/T)$ on $1/T$ for the mechanism of protein denaturation with one irreversible step at various values of the temperature scanning rate v.

It is also of interest if we calculate the Q values evolved to different temperatures the plots $(1 - Q/Q_t)^r$ versus temperature can be constructed. For the denaturation model under discussion, the theoretical dependence of $(1 - Q/Q_t)^r$ on T has the following form:

$$(1 - Q/Q_t)^r = \exp\left\{-\int_{T_0}^{T} \exp\left[\frac{E_a}{R}\left(\frac{1}{T^*} - \frac{1}{T}\right)\right] dT\right\} \quad (11)$$

Thus, in the case of validity of Eq. (1), the experimental data obtained for various values of the scanning rate must lie on the common curve in the coordinates $\{(1 - Q/Q_t)^r;\ T\}$.

4. New methods for estimation of Arrhenius equation parameters

The idea behind the use of several methods to determine the activation energy is to have at one's

disposal a convenient test for the validity of the one-step irreversible model with first-order kinetics (i.e., the agreement between the different values calculated for E_a). These methods have been successfully used for this purpose in several studies in recent literature [16–21]. It must be recognized, however, that some of these methods involve approximations, others involve potentially distorting transformations of the data and still others have limited accuracy, since they employ a single data point from each calorimetric profile. This suggests the advisability of exploring additional approaches to the analysis of DSC data in terms of the one-step (two-state) irreversible model. Four such new approaches are described below.

In principle, both the pre-exponential factor (A) and the activation energy may be calculated from the fitting of Eq. (9) to the experimental data. However, values of A and E_a are interrelated owing to compensatory effect [22], and this circumstance hampers fitting. Therefore, we propose to use T^* as a parameter for the estimation. It is expedient to calculate this parameter by the linear least square method using the equation:

$$1/T = 1/T^* - \ln\left[\upsilon C_p^{ex}/(Q_t - Q)\right]/(E_a/R) \quad (12)$$

i.e., using $\ln\left[\upsilon C_p^{ex}/(Q_t - Q)\right]$ as an independent variable and $1/T$ as dependent one. In this case, the T^* value can be estimated with significantly higher accuracy than $\ln A$ from linear regression using Eq. (9) because dispersion of variable $1/T$ is much less than dispersion of variable $\ln\left[\upsilon C_p^{ex}/(Q_t - Q)\right]$. Values of E_a calculated by using Eqs. (9) and (12) do not practically differ in the ranges of accuracy of their estimation.

One of disadvantages of the methods for the Arrhenius equation parameter estimation based on using Eqs. (9) and (12) is the high sensitivity of results to distortions on the initial and final parts of the C_p^{ex} versus temperature profile. For this reason, a limited range of experimental points is usually employed. Another disadvantage is the following. To estimate the parameters, one should minimize deviations not from the experimental curve, but from its linear anamorphosis. As a result, the theoretical C_p^{ex} versus temperature profile calculated with the parameters estimated by these methods coincides poorly with the experimental curve near the point of maximum.

In principle, the above disadvantages could be avoided if the parameters are estimated from the nonlinear, least-squares fitting of Eq. (8) to the experimental C_p^{ex} versus temperature profile. This, however, requires the preliminary calculation of the values of Q and Q_t (as in the case of the methods based on using Eqs. (9) and (12)). It should be noted that the distortions on the initial and final parts of the C_p^{ex} versus temperature profile may result in the appearance of systematic errors in calculation of Q and Q_t values. Besides, the variable Q is used as independent variable although, really, it is calculated from the variable C_p^{ex}.

We also consider a new method based on the nonlinear, least-squares fitting of Eq. (10) to the $[\mathrm{d}(\ln C_p^{ex})/\mathrm{d}(1/T)]$ versus $1/T$ profile. This method avoids integration because Eq. (10) does not include the parameter Q_t or variable Q. However, the method is again sensitive to distortions on the initial and final parts of the C_p^{ex} versus temperature profile.

Possibly, the best approach would be the nonlinear, least-squares fitting of Eq. (7) to the original excess heat capacity profiles. This method should be practically insensitive to distortions on the initial and final parts of the C_p^{ex} versus temperature profile. It does not use the variable Q, whereas the parameter Q_t can be considered as estimated. In addition, the

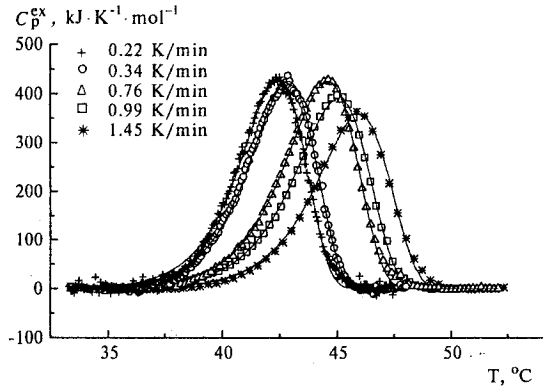

Fig. 2. Temperature dependence of excess heat capacity (C_p^{ex}) obtained by Kreimer et al. [23] for *T. californica* acetylcholinesterase in 0.1 M NaCl–10 mM Na-phosphate, pH 7.3, at different scanning rates. (————) best fit by using Eq. (7).

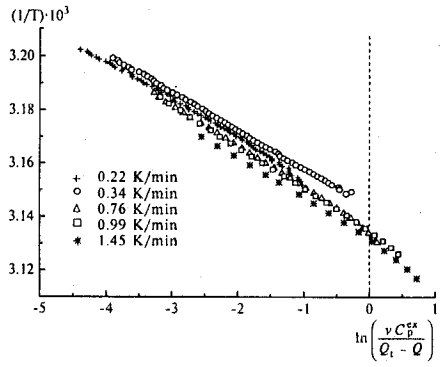

Fig. 3. Dependences of $1/T$ on ln $[\upsilon C_p^{ex}/(Q_t - Q)]$ for *T. californica* acetylcholinesterase calculated from the experimental data by Kreimer et al. [23].

integral in Eq. (7) can be calculated with more accuracy than Q, using any step on temperature axis.

5. Analysis of DSC curves

In this section, we will illustrate the approaches proposed above with the analysis of recently published DSC data corresponding to the irreversible thermal denaturation of acetylcholinesterase from *T. californica* [23], cellulase from *S. halstedii* JM8 [24], and lentil lectin [25].

5.1. Methods

To estimate Arrhenius equation parameters by methods based on using Eqs. (7) and (8), all experimental points were used. To estimate Arrhenius equation parameters by methods based on using Eqs. (10) and (12), the experimental points in the range of Q/Q_t values from 5 to 95% were used.

To estimate Arrhenius equation parameters by methods based on using Eqs. (8) and (10), software Microcal Origin, version 3.5 (Microcal Software) was used. To estimate Arrhenius equation parameters by methods based on using Eqs. (7) and (12), we used an original program for IBM-compatible computer based on Nelder and Meed's minimization algorithm [26]. Standard error of parameter estimation was calculated as described by Aivazyan et al. [27]. Correlation coefficient (r) for methods based on using Eq. (7) was calculated according the equation:

$$r = \sqrt{1 - \sum_{i=1}^{n} \left(y_i - y_i^{calc}\right)^2 \Big/ \sum_{i=1}^{n} \left(y_i - y_i^{m}\right)^2} \quad (13)$$

where y_i and y_i^{calc} are experimental and calculated values of C_p^{ex}, y_i^m is the mean of experimental values of C_p^{ex}, n is the number of points.

5.2. Acetylcholinesterase

Fig. 2 shows the C_p^{ex} versus temperature profiles obtained at various scanning rates for acetylcholinesterase from *T. californica* by Kreimer et al. [23]. In accordance with Eqs. (10) and (12), these experimental data were presented in coordinates $\{1/T;\ \ln [\upsilon C_p^{ex}/(Q_t - Q)]\}$ (Fig. 3) and $\{d(\ln C_p^{ex})/d(1/T)\}$ (Fig. 4). The parameters of the Arrhenius equation calculated using these equations are given in Table 1. This table contains also the values of parameters estimated by fitting of the experimental C_p^{ex} versus temperature profiles to Eqs. (7) and (8).

The estimation of E_a values by methods based on using Eqs. (7) and (10) (i.e., by methods which dispense with the need for using the variable Q), and by methods based on using Eqs. (8) and (12) (i.e., by methods using the variable Q), give the coincident

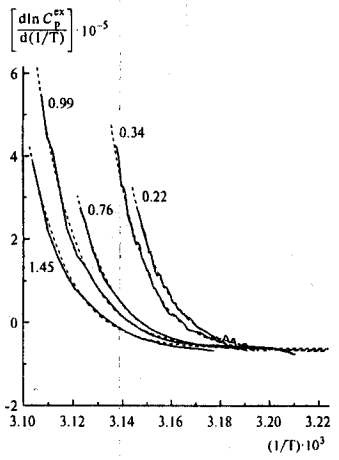

Fig. 4. Dependences of $d(\ln C_p^{ex})/d(1/T)$ on $1/T$ for *T. californica* acetylcholinesterase calculated from experimental data presented by Kreimer et al. [23]. Dotted lines are drawn in accordance with theoretical Eq. (10). Numbers near the curves refer to the scanning rate in K/min.

Table 1
Arrhenius equation parameter estimates for acetylcholinesterase from *T. californica*[a]

Method based on	Parameter[b]	Temperature scanning rate, K/min				
		0.22	0.34	0.76	0.99	1.45
Eq. (12)	E_a, kJ/mol	566.8 ± 4.2	582.8 ± 1.8	525.4 ± 4.4	527.2 ± 2.8	523.6 ± 8.2
	T^*, K	318.5 ± 0.03	318.1 ± 0.01	319.0 ± 0.02	319.0 ± 0.01	319.4 ± 0.03
Eq. (8)	E_a, kJ/mol	555.4 ± 4.8	583.4 ± 3.3	510.9 ± 5.3	522.7 ± 2.8	511.5 ± 6.2
	T^*, K	318.5 ± 0.02	318.1 ± 0.01	319.0 ± 0.01	319.0 ± 0.01	319.4 ± 0.01
Eq. (10)	E_a, kJ/mol	595.9 ± 7.0	587.7 ± 4.3	535.8 ± 4.2	526.0 ± 3.3	517.1 ± 11.5
	T^*, K	318.2 ± 0.02	318.0 ± 0.01	318.9 ± 0.01	318.9 ± 0.01	319.3 ± 0.02
Eq. (7)	E_a, kJ/mol	595.5 ± 3.7	586.1 ± 2.9	543.9 ± 3.1	531.8 ± 2.2	538.6 ± 4.8
	T^*, K	318.2 ± 0.02	318.1 ± 0.02	318.9 ± 0.02	319.0 ± 0.01	319.3 ± 0.02
	r[c]	0.9974	0.9986	0.9990	0.9996	0.9987

[a]0.1 M NaCl–10 mM Na-phosphate buffer, pH 7.3.
[b]The estimates ± standard errors are given.
[c]Correlation coefficient (r) is calculated by Eq. (13).

results. At the same time, for the scanning rates of 0.22, 0.76 and 1.45 K/min, the differences between the estimates, calculated by each pair of methods, are significant ($P < 0.05$ with the Student criterion). It should be noted that for the rates of 0.99 and 0.34 K/min, both pairs of methods give similar values of E_a, the accuracy of parameter estimations being the highest for these two rates for each method as well.

Regarding the estimates of E_a calculated for different scanning rates, these estimates do not practically differ for three high rates, whereas for the two lower rates, the E_a values are significantly higher ($P < 0.001$). (Note that there is a good agreement between the estimates of E_a calculated for the two lower rates by using the methods in which the variable Q is not used.)

Conclusions similar to those described above for E_a are reached for the parameter T^*.

Thus, application of Eq. (1) to analysis of DSC data for acetylcholinesterase gives different estimates of Arrhenius equation parameters for high and low scanning rates. In particular, this result is further demonstrated in Fig. 5 where the dependences of $\ln C_p^{ex}$ on $1/T$ combined in the maximum points are presented. As can be seen, the experimental points corresponding to $\ln C_p^{ex}$ versus $1/T$ profiles at various v values do not lie on a common curve. I

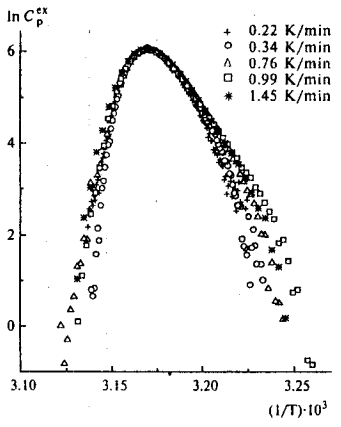

Fig. 5. Dependences of $\ln C_p^{ex}$ on $1/T$ for *T. californica* acetylcholinesterase combined in the maximum points with the corresponding dependence obtained at $v = 0.22$ K/min.

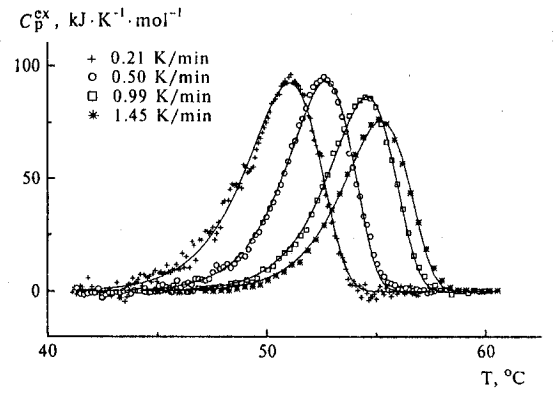

Fig. 6. Temperature dependence of excess heat capacity (C_p^e obtained by Garda-Salas et al. [24] for cellulase from *S. halstec* JM8 in 0.1 M phosphate, pH 6, at different scanning rat (————) best fit by using Eq. (7).

Table 2
Arrhenius equation parameter estimates for cellulase from *S. halstedii* JM8[a]

Method based on	Parameter[b]	Temperature scanning rate, K/min			
		0.21	0.50	0.99	1.45
Eq. (12)	E_a, kJ/mol	529.8 ± 6.2	588.0 ± 6.6	594.4 ± 5.2	586.7 ± 10.6
	T^*, K	327.6 ± 0.06	327.6 ± 0.04	328.4 ± 0.02	328.6 ± 0.04
Eq. (8)	E_a, kJ/mol	537.6 ± 4.0	568.6 ± 4.9	581.8 ± 4.2	567.5 ± 7.5
	T^*, K	327.5 ± 0.02	327.6 ± 0.01	328.4 ± 0.01	328.5 ± 0.01
Eq. (10)	E_a, kJ/mol	516.0 ± 43.8	578.6 ± 7.4	590.6 ± 6.4	588.5 ± 12.9
	T^*, K	327.7 ± 0.21	327.5 ± 0.02	328.3 ± 0.01	328.5 ± 0.02
Eq. (7)	E_a, kJ/mol	529.8 ± 4.3	595.8 ± 4.3	596.5 ± 4.1	595.7 ± 5.8
	T^*, K	327.6 ± 0.04	327.4 ± 0.02	328.4 ± 0.02	328.5 ± 0.02
	r[c]	0.9960	0.9982	0.9990	0.9987

[a]0.1 M phosphate, pH 6.
[b]The estimates ± standard errors are given.
[c]Correlation coefficient (r) is calculated by Eq. (13).

accordance with the values of E_a given in Table 1 in the temperature range where T is lower than T_m (the temperature corresponding to the maximal value of C_p^{ex}), a divergence between points at low and high v values occurs. This fact indicates that Eq. (1) does not operate strictly for acetylcholinesterase from *T. californica*.

5.3. Cellulase

Fig. 6 shows the C_p^{ex} versus temperature profiles obtained at different scanning rates for cellulase from *S. halstedii* JM8 by Garda-Salas et al. [24]. The parameters of Arrhenius equation calculated by using Eqs. (7), (8), (10) and (12) are given in Table 2. The values of E_a calculated for three high scanning rates are very close (especially for the method based on using Eq. (7)). The estimate of E_a for the low rate (0.21 K/min) is significantly smaller than those for other rates. In this aspect, cellulase differs from acetylcholinesterase, for which maximal estimates were obtained for low scanning rates.

The shape of combined dependences of ln C_p^{ex} on $1/T$ for cellulase (Fig. 7) also demonstrates the differences between the E_a values for low and high scanning rates.

However, it is interesting that the estimate of parameter T^* for the rate of 0.21 K/min does not practically differ from that for the rate of 0.50

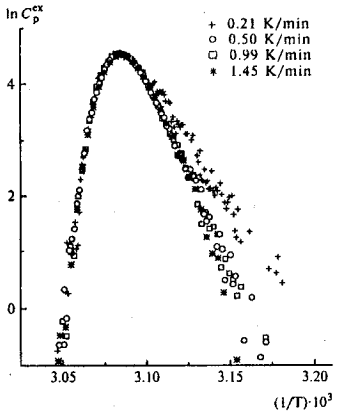

Fig. 7. Dependences of ln C_p^{ex} on $1/T$ for cellulase from *S. halstedii* JM8 combined in the maximum points with the corresponding dependence obtained at $v = 0.21$ K/min.

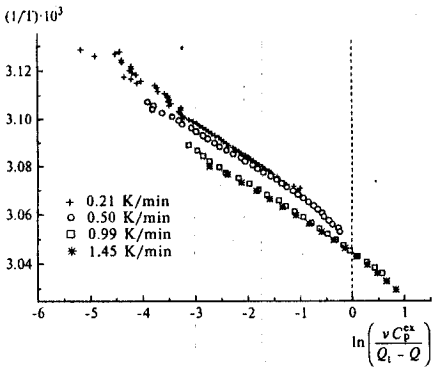

Fig. 8. Dependences of $1/T$ on ln $[vC_p^{ex}/(Q_t - Q)]$ for cellulase from *S. halstedii* JM8 calculated from the experimental data by Garda-Salas et al. [24].

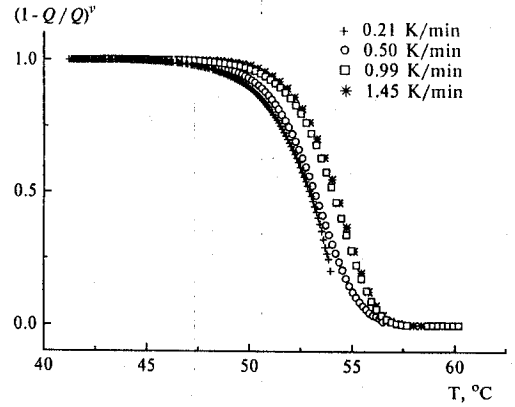

Fig. 9. Dependences of $(1 - Q/Q_t)^{\nu}$ on temperature for cellulase from *S. halstedii* JM8 calculated from experimental data presented by Garda-Salas et al. [24].

K/min, whereas for two higher rates, these estimates are significantly higher and also coincide with each other. Figs. 8 and 9 where experimental data are presented in coordinates $\{1/T;\ \ln [\nu C_p^{ex}/(Q_t - Q)]\}$ and $\{(1 - Q/Q_t)^{\nu};\ T\}$, respectively, demonstrate closeness of the values of parameter T^* both for a pair of low rates and that of high rates.

Thus, the estimates of both parameters are close only for the rates of 0.99 and 1.45 K/min.

5.4. Lectin

Fig. 10 shows the C_p^{ex} versus temperature profiles obtained at different scanning rates for lentil lectin

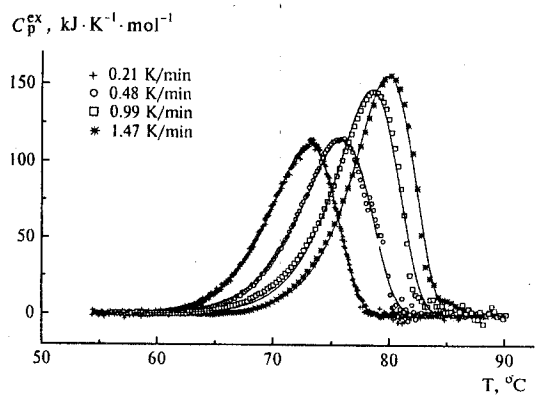

Fig. 10. Temperature dependence of excess heat capacity (C_p^{ex}) obtained by Shnyrov et al. [25] for lentil lectin in 10 mM potassium phosphate, pH 7.4, at different scanning rates. (————) best fit by using Eq. (7).

by Shnyrov et al. [25]. The estimates of Arrhenius equation parameters are given in Table 3. As in two cases described above, differences in the estimates for different methods are less significant than those for different scanning rates. The methods based on using Eqs. (7), (10) and (12) give similar results for all rates besides 1.47 K/min.

However, all methods give significantly different estimates of E_a ($P < 0.05$) for different scanning rates. The lowest value of the parameter is calculated for a middle rate of 0.48 K/min. Note that, in this case, the E_a versus scanning-rate dependence appears to pass through a minimum at a scanning rate of about 0.5 K/min.

6. Effect of possible baseline distortions

In principle, the differences between the estimates of the kinetic parameters (Tables 1–3) could be due to systematic instrumental distortions, such as instrumental baseline uncertainties, rather than to actual deviations from the one-step (two-states) irreversible model with first-order kinetics. In order to rule out this possibility, we will consider in this section the effect of baseline distortions on the parameters derived from the kinetic analysis of the DSC transitions.

First of all, we believe that the Takahashi and Sturtevant [28] procedure of chemical baseline tracing is quite correct for the models of two-state transition (reversible or irreversible). Taking the native state as reference, the Takahashi and Sturtevant chemical baseline is given by $\gamma_D \Delta C_p^{ex}$, where γ_D is the mole fraction of the denaturated state and ΔC_p^{ex} is the denaturation heat capacity change. If we assume that ΔC_p^{ex} can be taken as a constant within the comparatively narrow temperature range of the DSC transition, then the pre- and post-transition heat capacity levels will be parallel and the extrapolation of these levels to the temperature at which $\gamma_D = 1/2$ ($T = T_{1/2}$) would yield the ΔC_p^{ex} value. The Takahashi and Sturtevant chemical baseline looks like a sigmoidal curve with a value of $\Delta C_p^{ex}/2$ (taking the native state as a reference) at temperature $T_{1/2}$.

We believe that the real problem is related to possible instrumental baseline distortions. If we are

Table 3
Arrhenius equation parameter estimates for lentil lectin[a]

Method based on	Parameter[b]	Temperature scanning rate, K/min			
		0.21	0.48	0.99	1.47
Eq. (12)	E_a, kJ/mol	359.9 ± 0.8	347.3 ± 2.0	373.9 ± 3.2	389.7 ± 3.1
	T^*, K	353.5 ± 0.02	354.4 ± 0.05	354.3 ± 0.06	354.6 ± 0.04
Eq. (8)	E_a, kJ/mol	348.1 ± 2.0	339.8 ± 2.4	358.0 ± 5.2	378.3 ± 4.8
	T^*, K	353.8 ± 0.04	354.6 ± 0.04	354.6 ± 0.05	354.8 ± 0.03
Eq. (10)	E_a, kJ/mol	355.8 ± 3.4	329.5 ± 12.8	370.8 ± 6.7	386.5 ± 3.4
	T^*, K	353.6 ± 0.06	354.8 ± 0.21	354.4 ± 0.06	354.7 ± 0.03
Eq. (7)	E_a, kJ/mol	360.9 ± 1.0	345.6 ± 2.5	384.0 ± 3.8	402.1 ± 3.5
	T^*, K	353.5 ± 0.03	354.4 ± 0.06	354.3 ± 0.05	354.5 ± 0.04
	r[c]	0.9988	0.9970	0.9961	0.9980

[a] 10 mM potassium phosphate, pH 7.4.
[b] The estimates ± standard errors are given;
[c] Correlation coefficient (r) is calculated by Eq. (13).

using a slightly wrong instrumental baseline, after subtraction of it, the pre- and post-transition levels will not appear parallel and their extrapolation to $T_{1/2}$ overestimates or underestimates the true ΔC_p^{ex} value.

Let us consider first the overestimation case. Suppose that the heat capacity levels do not appear parallel in such a way that the denaturation heat capacity change we get from the extrapolation to $T_{1/2}$ is 1.5 times larger than what it should be; that is, we get $1.5\Delta C_p^{ex}$ instead of ΔC_p^{ex} (an overestimation of 50%). Then, the chemical baseline will have a value of $0.75\Delta C_p^{ex}$ at $T_{1/2}$.

We consider now the underestimation case. Suppose that the heat capacity levels do not appear parallel in such a way the denaturation heat capacity change we obtain from their extrapolation to $T_{1/2}$ is half what is should be, that is, we get $\Delta C_p^{ex}/2$ instead of ΔC_p^{ex} (an underestimation of 50%). In this case, the chemical baseline has a value of $\Delta C_p^{ex}/4$ at $T_{1/2}$.

Thus, the effect of using slightly wrong instrumental baselines may be modeled by using distorted chemical baselines. It is reasonable to suppose over- and underestimation of 50% considered above as the upper and lower limits of distortions. We have found that the upper-limit distorted chemical baseline may be modeled as $\gamma_D^{0.415}\Delta C_p^{ex}$ and the lower-limit distorted chemical baseline as $\gamma_D^2\Delta C_p^{ex}$. It is also reasonable to assume the value of ΔC_p^{ex} for modeling as $C_{p,\,max}^{ex}/10$, where $C_{p,\,max}^{ex}$ is the excess heat capacity at the maximum of the transition.

Taking into consideration that $\gamma_D = Q/Q_t$, we obtain the function

$$(C_{p,\,max}^{ex}/10)\left[Q/Q_t - (Q/Q_t)^{0.415}\right] \qquad (14)$$

for the upper-limit distortion and the function

$$(C_{p,\,max}^{ex}/10)\left[Q/Q_t - (Q/Q_t)^2\right] \qquad (15)$$

for the lower-limit distortion. Adding these functions to an original C_p^{ex} versus temperature profile gives two distorted profiles which can be analyzed by kinetic methods.

Of course, this procedure is empirical; however, it produces distortions similar to those often found in experimental thermograms, and therefore, allows us to obtain qualitative estimates of the effect of baseline distortions on the parameters derived from the kinetic analysis.

Two distorted C_p^{ex} versus temperature profiles were obtained for all thirteen original profiles described in Section 5, and the Arrhenius equation parameters were calculated by using Eqs. (7) and (12). For the low-limit distortion profiles, the values of E_a differ from the corresponding original profiles by less than 0.7%, and values of T^* differ by less than 0.01%.

For the upper-limit distortion profiles, differences are higher. The values of E_a calculated for these profiles by using Eq. (7) were higher than that for the original profiles by 2.2–3.6%. The values of E_a calculated by using Eq. (12) were higher than for the

original profiles by 0.4–4.1%. Such differences are compatible with the differences between the values of E_a calculated by different methods but they are less than the maximum differences between the values of E_a calculated for C_p^{ex} versus temperature profiles obtained at different scanning rate (about 10%).

The values of T^* for the upper-limit distortion profiles differ from the corresponding original profiles by less than 0.05%.

Thus, possible distortions introduced by instrumental baseline uncertainties could not affect the main results of the present work.

7. Discussion

Eq. (1) is the simplest model of irreversible thermal denaturation of proteins. Therefore, the analysis of DSC data of a protein undergoing irreversible thermal denaturation should begin with checking whether experimental data satisfy the one-step model.

One can start the analysis of DSC data with plotting of $1/T$ versus $\ln [vC_p^{ex}/(Q_t - Q)]$ for a single scanning rate. If the data satisfy the model, experimental points on this plot are approximated by a straight line (at least in the range of Q/Q_t values from 5 to 95%).

However, such an approach is insufficient. To prove the validity of the model, data for different scanning rates should be used. In this case, linear anamorphosis in coordinates $\{1/T; \ln [vC_p^{ex}/(Q_t - Q)]\}$ is also useful: if the model is valid, the points corresponding to all the rates should lie on a common straight line. Analogous criterion includes plotting $(1 - Q/Q_t)^r$ versus T.

Using coordinates $\{\ln C_p^{ex}; 1/T\}$ gives another criterion. The identity of the shape of $\ln C_p^{ex}$ versus $1/T$ curves obtained at various values of the scanning rate testifies to the validity of one-step irreversible model.

The results of our analysis show that the coordinates $\{\ln C_p^{ex}; 1/T\}$ may clearly demonstrate discrepancies in E_a values for different scanning rates, whereas the coordinates $\{1/T; \ln [vC_p^{ex}/(Q_t - Q)]\}$ as well as the coordinates $\{(1 - Q/Q_t)^r; T\}$ are applicable for demonstration of discrepancies in the values of parameter T^* (see, for example, Figs. 7–9).

The more reliable checking of the model is to estimate the Arrhenius equation parameters for different scanning rates by methods based on using Eqs. (7), (10) and (12). If the model is valid, these estimates should not diverge considerably. Significance of the divergences may be estimated by the ordinary statistical methods (for example, by Student criterion).

Analysis of DSC data for acetylcholinesterase, cellulase, and lectin given in the present work shows that thermal denaturation of all these proteins do not strictly follow the one-step irreversible model (Eq. (1)). It is evident that some additional (reversible or irreversible) steps should be taken into consideration. The most attractive is the Lumry and Eyring mechanism [29]

$$N \rightleftarrows U \rightarrow D \qquad (16)$$

This mechanism involves a reversible unfolding step followed by an irreversible denaturation step. The theoretical analysis of C_p^{ex} versus temperature profiles for denaturation of proteins in accordance to the Lumry and Eyring mechanism was carried out by Sanchez-Ruiz [11] and Lepock et al. [30]. Milardi et al. [31], La Rosa et al. [32] and Tello-Solis and Hernandez-Arana [33] made an attempt to describe quantitatively the experimental C_p^{ex} versus temperature profile using the Lumry and Eyring mechanism with fast equilibrating $N \rightleftarrows U$ step.

A final point must be made, however. The two-state irreversible model appears as a limiting case of several more realistic models [10–12]. As such, it must be considered as an ideal case and, even in cases of good general adherence to the model, we can expect deviations to be revealed by a careful data analysis. Whether such deviations are to be considered significant or not depends on several factors, among them the general purpose of the analysis. For instance, one of the main stimulus for the original development of the two-state model of irreversible denaturation [16] was to provide researchers with practical tests to determine whether the analysis of DSC thermograms on the basis of equilibrium thermodynamics was permissible or not. From this point of view, small deviations from the model are immaterial; that is, even a merely approximate adherence to the model shows clearly that the

analysis of the calorimetric thermograms on the basis of equilibrium thermodynamics is not permissible. Of course, from a different point of view, deviations might be important as a starting point for more complex analyses addressed to characterize possible intermediate states in the denaturation process.

Acknowledgements

We are grateful to Dr. D.R. Davydov for the assistance in preparing the computer program. The study was funded by grants 96-04-50819 and 96-04-10016C from the Russian Foundation for Fundamental Research.

References

[1] E. Freire, R.L. Biltonen, Biopolymers 17 (1978) 463.
[2] P.L. Privalov, Adv. Protein Chem. 33 (1979) 167.
[3] P.L. Privalov, Adv. Protein Chem. 35 (1982) 1.
[4] V.V. Filimonov, S.A. Potekhin, S.V. Matveev, P.L. Privalov, Mol. Biol. (Moscow) 16 (1982) 551, (In Russian).
[5] P.L. Mateo, in: R. da Silva (Ed.), Thermochemistry and Its Applications to Chemical and Biochemical Systems, Reidel, Dordrecht, 1984, p. 541.
[6] P.L. Privalov, S.A. Potekhin, Methods in Enzymology, Vol. 131, Academic Press, New York, 1986, p. 4.
[7] J.M. Sturtevant, Annu. Rev. Phys. Chem. 38 (1987) 463.
[8] J.M. Sanchez-Ruiz, P.L. Mateo, Cell Biol. Rev. 11 (1987) 15.
[9] P.L. Privalov, Annu. Rev. Biophys. Chem. 18 (1989) 47.
[10] E. Freire, W.W. van Osdol, O.L. Mayorga, J.M. Sanchez-Ruiz, Annu. Rev. Biophys. Chem. 19 (1990) 159.
[11] J.M. Sanchez-Ruiz, Biophys. J. 61 (1992) 921.
[12] J.M. Sanchez-Ruiz, Proteins: structure, function, and engineering, in: B.B. Biswas, S. Roy (Eds.), Subcellular Biochemistry, Vol. 24, Plenum, New York, 1995, p. 133.
[13] J.F. Brandts, C.Q. Hu, L.-N. Lin, M.T. Mas, Biochemistry 28 (1989) 8588.
[14] G. Ramsay, E. Freire, Biochemistry 29 (1990) 8677.
[15] A.M. Klibanov, T.J. Ahern, in: D.L. Oxender, C.F. Fox (Ed.), Protein Engineering, Alan R. Liss, New York, 1987, p. 213.
[16] J.M. Sanchez-Ruiz, J.L. Lopéz-Lacomba, M. Cortijo, P.L. Mateo, Biochemistry 27 (1988) 1648.
[17] J.M. Sanchez-Ruiz, J.L. Lopez-Lacomba, P.L. Mateo, M. Vilanova, M.A. Serra, F.X. Aviles, Eur. J. Biochem. 176 (1988) 225.
[18] M. Guzmán-Casado, A. Parody-Morreale, P.L. Mateo, J.M. Sanchez-Ruiz, Eur. J. Biochem. 188 (1990) 181.
[19] P.E. Morin, D. Diggs, E. Freire, Biochemistry 29 (1990) 781.
[20] J.R. Lepock, A.M. Rodahl, C. Zhang, M.L. Heynen, B. Waters, K.-H. Cheng, Biochemistry 29 (1990) 681.
[21] F. Conejero-Lara, J.M. Sanchez-Ruiz, P.L. Mateo, F.J. Burgos, J Vendrell, F.X. Avilés, Eur. J. Biochem. 200 (1991) 663.
[22] B.I. Sukhorukov, G.I. Likhtenstein, Biofizika 10 (1965) 935, (In Russian).
[23] D.I. Kreimer, V.L. Shnyrov, E. Villar, I. Silman, L. Weiner, Protein Sci. 4 (1995) 2349.
[24] A.L. Garda-Salas, R.I. Santamarća, M.J. Marcos, G.G. Zhadan, E. Villar, V.L. Shnyrov, Biochem. Mol. Biol. Int. 38 (1996) 161.
[25] V.L. Shnyrov, M.J. Marcos, E. Villar, Biochem. Mol. Biol. Int. 39 (1996) 647.
[26] J.A. Nelder, R. Meed, Comput. J. 7 (1965) 308.
[27] S.A. Aivazyan, I.S. Yenyukov, L.D. Meshalkin, Applied Statistics. Study of Relationships, Finansy i Statistika, Moscow, 1985 (In Russian).
[28] K. Takahashi, J.M. Sturtevant, Biochemistry 20 (1981) 6185.
[29] R. Lumry, H. Eyring, J. Phys. Chem. 58 (1954) 110.
[30] J.R. Lepock, K.P. Ritchie, M.C. Kolios, A.M. Rodahl, K.A. Heinz, J. Kruuv, Biochemistry 31 (1992) 12706.
[31] D. Milardi, C. La Rosa, D. Grasso, Biophys. Chem. 52 (1994) 183.
[32] C. La Rosa, D. Milardi, D. Grasso, R. Guzzi, L. Sportelli, J. Phys. Chem. 99 (1995) 14864.
[33] S.R. Tello-Solis, A. Hernandez-Arana, Biochem. J. 311 (1995) 969.